Advanced bioactive glue tethering Lubricin/PRG4 to promote integrated healing of avascular meniscus tears

Solaiman Tarafder [a], Jaskirti Ghataure [a], David Langford [a], Rachel Brooke [a], Ryunhyung Kim [a], Samantha Lewis Eyen [a], Julian Bensadoun [a], Jeffrey T. Felix [a], James L. Cook [b], Chang H. Lee [a,*]

[a] Regenerative Engineering Laboratory, Columbia University Medical Center, 630 W. 168 St. – VC12-212, New York, NY, 10032, USA
[b] Thompson Laboratory for Regenerative Orthopaedics, Missouri Orthopedic Institute, University of Missouri, 1100 Virginia Avenue, Columbia, MO, 65212, USA

ARTICLE INFO

ABSTRACT

Meniscus injuries are extremely common with approximately one million patients undergoing surgical treatment annually in the U.S. alone, but no regenerative therapy exist. Previously, we showed that controlled applications of connective tissue growth factor (CTGF) and transforming growth factor beta 3 (TGFβ3) via fibrin-based bio-glue facilitate meniscus healing by inducing recruitment and stepwise differentiation of synovial mesenchymal stem/progenitor cells. Here, we first explored the potential of genipin, a natural crosslinker, to enhance fibrin-based glue's mechanical and degradation properties. In parallel, we identified the harmful effects of lubricin on meniscus healing and investigated the mechanism of lubricin deposition on the injured meniscus surface. We found that the pre-deposition of hyaluronic acid (HA) on the torn meniscus surface mediates lubricin deposition. Then we implemented chemical modifications with heparin conjugation and CD44 on our bioactive glue to achieve strong initial bonding and integration of lubricin pre-coated meniscal tissues. Our data suggested that heparin conjugation significantly enhances lubricin-coated meniscal tissues. Similarly, CD44, exhibiting a strong binding affinity to lubricin and hyaluronic acid (HA), further improved the integrated healing of HA/lubricin pre-coated meniscus injuries. These findings may represent an important foundation for developing a translational bio-active glue guiding the regenerative healing of meniscus injuries.

1. Introduction

Approximately one million patients undergo meniscus repair or partial meniscectomy each year in the U.S [1,2]. Tears in the vascularized outer third region of the meniscus have a high rate of functional healing after surgical repair. In contrast, tears in the inner avascular region have low rates of functional healing after repair due to poor intrinsic healing capabilities. Failure to achieve functional meniscus healing frequently results in tear propagation, meniscus deterioration, and osteoarthritis of the affected knee [3–5]. Despite the prevalence, quality of life impact, and health care burden of meniscus injuries, there is no clinically applicable treatment to reliably induce seamless healing of avascular meniscus tears. Various bioengineering and regenerative strategies have been tested to improve the healing of avascular meniscus injuries, including biomaterial-based glues, stem/progenitor cells, and/or bioactive cues [6–10]. Delivery of autologous mesenchymal

stem/progenitor cells (MSCs) improved meniscus healing to some degree in rats, sheep, and mini-pigs [10–13]. Recently, a mobilization of cartilage progenitor cells (CPC) with CXCR4 modification improved the healing of meniscus tears [14]. Chemotactic cues and/or softening cell nuclei were also implemented to improve meniscus healing by promoting endogenous cell migration [15]. In parallel, a growing body of studies investigated various biomaterial grafts or tissue glues to promote avascular meniscus healing [16,17]. However, functional healing of avascular meniscus tears with a successful recapitulation of biochemical composition and biomechanical properties has yet to be achieved.

Our group has recently devised an *in-situ* tissue engineering approach for the regenerative healing of avascular meniscus tears [8,9]. We have reported that a single application of connective tissue growth factor (CTGF)-loaded fibrin glue mixed with poly(lactic-co-glycolic acids) (PLGA) microspheres (µS)-encapsulating transforming growth factor beta 3 (TGFβ3) successfully recruited synovial mesenchymal

stem/progenitor cells (syMSCs) into a surgically-created avascular meniscus tear, followed by integrated healing with fibrocartilaginous tissue [8,9]. Despite promising outcomes in both *in vitro* and *in vivo* meniscus healing models, the previously used fibrin-based glue requires significant improvements to meet the physio-chemical needs for its applications for meniscus healing in large animal models and human patients. Fibrin is biocompatible and suitable for delivering CTGF and TGFβ3-μS as per our previous studies. However, its weak bonding strength and rapid degradation represent the translational hurdles of fibrin as a bio-glue facilitating musculoskeletal tissue healing [18]. Particularly for meniscus healing, intrasynovial fibrinolysis is a critical concern for the intra-articular application of fibrin glue [18]. To circumvent the issue, this study explored the potential of genipin, a natural crosslinker [19,20], in fortifying fibrin gel by improving the mechanical properties and slowing the degradation rate. Genipin has been widely used to crosslink various types of hydrogels with proven safety and biocompatibility [19,20].

In addition, we took consideration of lubricin into the design of bioactive glue for meniscus healing. Lubricin, also referred to as proteoglycan 4 (PRG4), is a surface-active mucinous glycoprotein abundant in the articular surfaces of cartilage and menisci, playing essential roles in providing frictionless joint movement [21–23]. An *in vitro* experiment showed that lubricin readily binds on the articular surface but not on a radially incised surface of cartilage explants [22,24]. In contrast, human biopsies from injured menisci revealed a notable expression of lubricin on the torn surface of menisci [25]. Due to the intrinsic nature of lubricin in preventing cell and protein adhesion [21], we hypothesized that lubricin coating on the torn surface of menisci may prevent tissue integration and healing. As human patients typically visit a physician days to weeks after an initial meniscus injury [26,27], the injured meniscus surface exposed to synovial fluids containing lubricin likely ends up with lubricin-deposition on the injured surfaces [25]. Thus, it is very important to mitigate the harmful effect of lubricin to achieve successful healing of lubricin-deposited meniscus injuries, especially at

the avascular inner zone. Beyond mitigation, here we explored strategies to further strengthen the bonding and integration of lubricin-infiltrated torn meniscus tissues by modifying the fibrin-based bioactive glue with heparin and CD44. Heparin conjugation was adopted due to the existence of heparin-binding domain at the N-terminal of lubricin [21,28], and CD44, a surface protein highly expressed in syMSCs and many other cell types, was selected based on its strong binding affinity to lubricin [29].

We first investigated the mechanism of lubricin binding on the torn meniscus surface and then the harmful effects of lubricin coating on engineered healing of avascular meniscus tears. Based on the findings, we modified our bioactive glue to further improve meniscus healing by tethering lubricin on the torn surface. As lubricin has been widely investigated in regard to its positive roles in the protection of the articular surface and delaying the onset of osteoarthritis [30,31], our study represents the first attempt to address the potentially harmful effects of lubricin infiltration on torn meniscus surface. This study has a notable significance for developing translational bioengineering approaches for the functional healing of avascular meniscus tears.

2. Results

2.1. Genipin-crosslinked fibrin glue improved mechanical and degradation properties at a dose dependent manner

Fibrin, despite being biocompatible and suitable for delivery of CTGF and TGFβ3-μS, has several limitations for application in pre-clinical large animal models and patients, including its weak bonding strength and rapid degradation. In particular, the intrasynovial fibrinolysis is a critical concern for intra-articular application of fibrin. To circumvent the issue, we applied genipin - a natural crosslinker - to fibrin gel (Fig. 1A). With increasing genipin concentration up to 10 mg/mL in 100 mg/mL fibrin, compressive moduli increased proportionally (Fig. 1B). Shear modulus and strength were also significantly increased by genipin
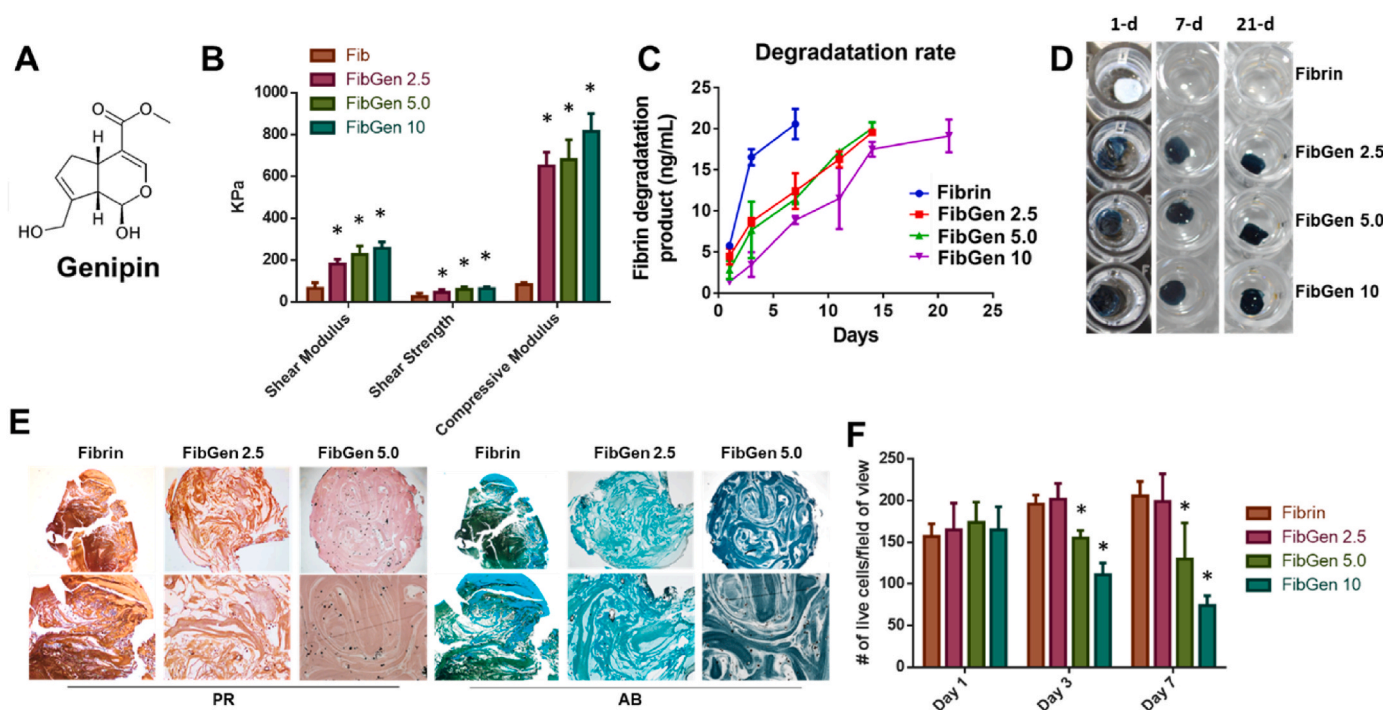

Fig. 1. Genipin is a natural crosslinker (A). Fibrin crosslinked with genipin (FibGen) at various doses (2.5 mg/mL, 5.0 mg/mL, and 10 mg/mL) showed significantly increased compressive and shear properties as compared to fibrin alone (B) (*:p < 0.0001 compared to Fib; n = 10 per group). In addition, genipin crosslinking significantly delayed *in vitro* degradation (C). Fibrin alone was fully degraded *in vitro* by 7 days in PBS, whereas FibGen maintained its volume by 21 days (D). However, genipin over 5 mg/mL resulted in too dense matrix leading to low cell viability (E) (PR: Picrosirius Red; AB: Alcian Blue). Quantitatively, live/dead assays showed significantly lower cell viabilities in FibGen 5.0 and FibGen 10 (*:p < 0.0001; n = 10 per group).

crosslinking (Fig. 1B). In addition, *in vitro* degradation of fibrin was significantly delayed with genipin crosslinking (Fig. 1C and D). Without genipin cross-linking, fibrin fully degraded in 7 days, not suitable for meniscus healing (Fig. 1C and D). Although they still degrade over time, FibGen showed significantly slower degradation with remaining structure by 21 days, making them more suitable as a bio-glue supporting meniscus healing (Fig. 1C &D). FibGen However, genipin over 5 mg/mL resulted in extremely dense matrix leading to cell death, significantly lowering cell viability when syMSCs (2 M/mL) were encapsulated within the gel, followed by undergoing fibrocartilaginous differentiation as per our established protocols [8,9]. By 4 weeks, FibGen 5.0 (5 mg/mL genipin) showed limited cellularity as compared to FibGen 2.5 and fibrin alone (Fig. 1E). Quantitatively, the live/dead assay showed significantly lower cell viabilities in FibGen 5.0 and FibGen 10 starting at day 3 (Fig. 1F) ($p < 0.0001$; n = 10 per group). Based on these findings, we selected 2.5 mg/mL of genipin to improve the mechanical and degradation properties of fibrin glue while maintaining cell viability and tissue formation. Prior to its application for meniscus healing model, we have tested the release kinetics of CTGF from FibGen (2.5 mg/mL genipin; 100 mg/mL fibrin). As compared to fibrin, FibGen showed a slower release of CTGF for a prolonged duration (Suppl. Fig. 1A). *In vitro* cell migration test showed that CTGF released from FibGen successfully induced migration of syMSCs comparable to fibrin (Suppl. Fig. 1B and C). To understand the mechanism of CTGF-induced migration of syMSCs, we targeted CD44 abundantly expressed on the cell surface (Suppl. Fig. 1D). When CD44 was neutralized using antibody, CTGF-induced migration of syMSCs was significantly reduced (Suppl. Fig. 1E) (*:$p < 0.0001$; n = 10 per group). This finding may suggest CD44 can be a receptor for CTGF in synovial MSCs, likely consistent with previous findings supporting CD44 as a cell surface receptor playing essential roles in cell migration [32].

2.2. Genipin-crosslinked fibrin glue promoted meniscus healing ex vivo

When tested in our well-established explant healing model [8,9,33], FibGen 2.5 loaded with 1000 ng/mL CTGF and 10 mg/mL TGFβ3 encapsulated in PLGA microspheres (μS) (2.5 μg per 250 mg PLGA) further facilitated integrated healing of avascular meniscus tears as compared to fibrin (Fig. 2A). By 4 weeks, FibGen 2.5 resulted in a high cellularity at the healing zone with improved tissue integration and matrix formation (Fig. 2A). Low magnification images further support the enhanced tissue integration over the defect with FibGen in comparison with fibrin (Suppl. Fig. 2A). Quantitative histomorphometry measurements were conducted for % of lengths of tissue disintegration (detached), apposition (integrated tissue but immature matrix), and integration (mature tissue integration) per a previous method [34], indicating significant improvement of tissue integration in FibGen 2.5 (Suppl. Fig. 2B).

Consistently, the tensile modulus and strength of healed menisci were significantly higher with FibGen 2.5 than fibrin (Fig. 2B) ($p < 0.001$; n = 5 per group). Modulus mapping using our well-established nanoindentation measurements [9] revealed an improvement in the distribution of effective indentation modulus (E_{Eff}) over the healing zone with FibGen 2.5 as compared to fibrin (Fig. 2C). Quantitatively, the average E_{Eff} in the healing zone was significantly higher with FibGen than fibrin (Fig. 2D) ($p < 0.0001$; n = 25 per group). The improved healing of avascular meniscus tears by genipin-crosslinking is likely associated with the enhanced initial bonding strength and slower degradation.

2.3. Detrimental effect of lubricin on meniscus healing

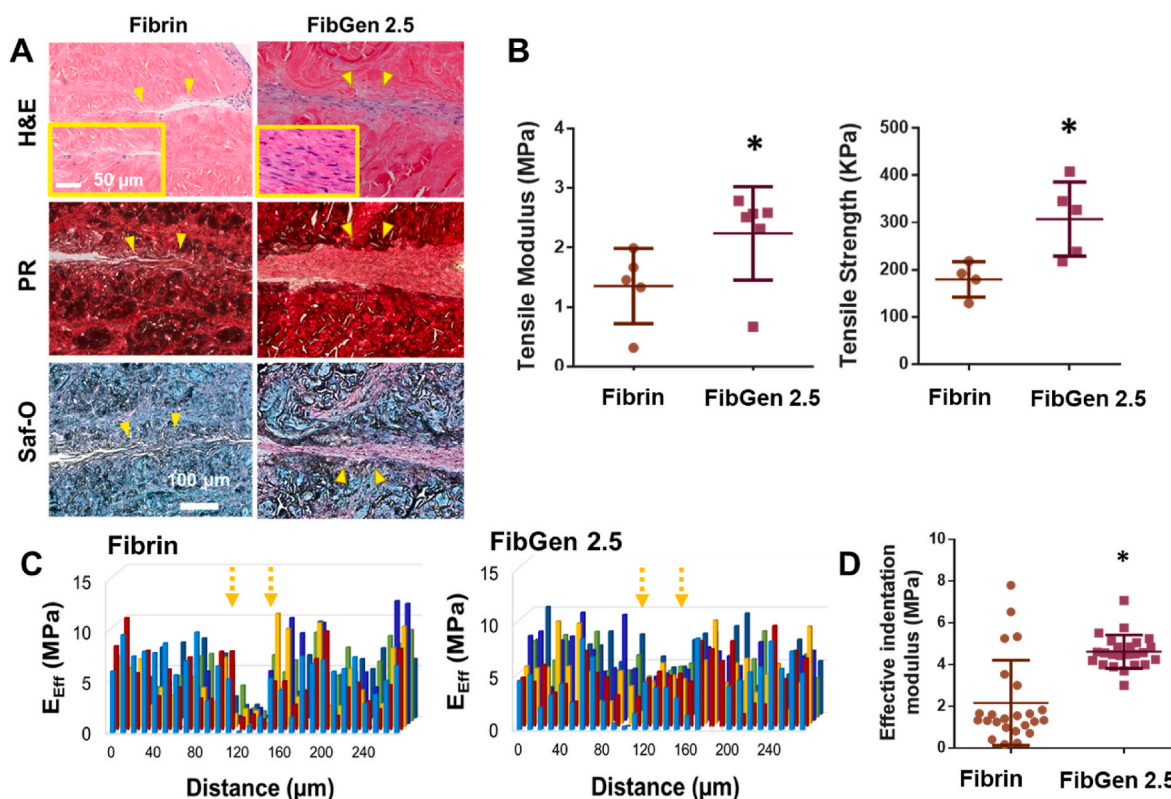Then we investigated effects of lubricin on the avascular meniscus

Fig. 2. In a bovine meniscus explant healing model via timely controlled delivery of CTGF and TGFβ3, FibGen significantly enhanced healing as compared to fibrin (A) (PR: Picrosirius Red; Saf-O: Safranin O; arrows indicate healing zone; boxes show high magnification). In addition, FibGen significantly increased tensile modulus and strength (B) (*:$p < 0.0001$; n = 5 per group). Effective indentation moduli (E_{Eff}) measured with nanoindentation show a more even distribution (C) and higher average value (D) with FibGen compared to fibrin (*:$p < 0.001$; n = 25 per group).

healing. Tissue samples from dogs with untreated meniscus injuries showed lubricin expression extended to the torn surface of meniscus rather than confined on the articular surface (Fig. 3A). Then we applied 1 M NaCl for 1 h to deplete surface lubricin (Fig. 3B). The dose and duration of NaCl were adopted from literature [22]. NaCl pre-treated meniscus explant showed a modest improvement in healing per histological evaluation (Fig. 3C). Modulus mapping by nanoindentation showed the distribution of indentation modulus in 220 μm × 120 μm area at 20 μm intervals (Fig. 3D), suggesting the improved healing of

NaCl pre-treated meniscus explants. Quantitatively, the effective indentation modulus (E_{Eff}) was significantly higher in NaCl pre-treated group compared to the control (Fig. 3E). To understand the effect of lubricin on meniscus healing, we established lubricin coating on the radially-cut surface of bovine menisci (Fig. 3F). Up to 24 h, the longer time of incubation at 37 °C in synovial fluids (SF) resulted in the more robust coating of lubricin in comparison with no coating & no antibody controls and incubation at 4 °C (Fig. 3F and G). Then we applied fibrin or FibGen with CTGF and TGFβ3-μS in our well-established *ex vivo* inner
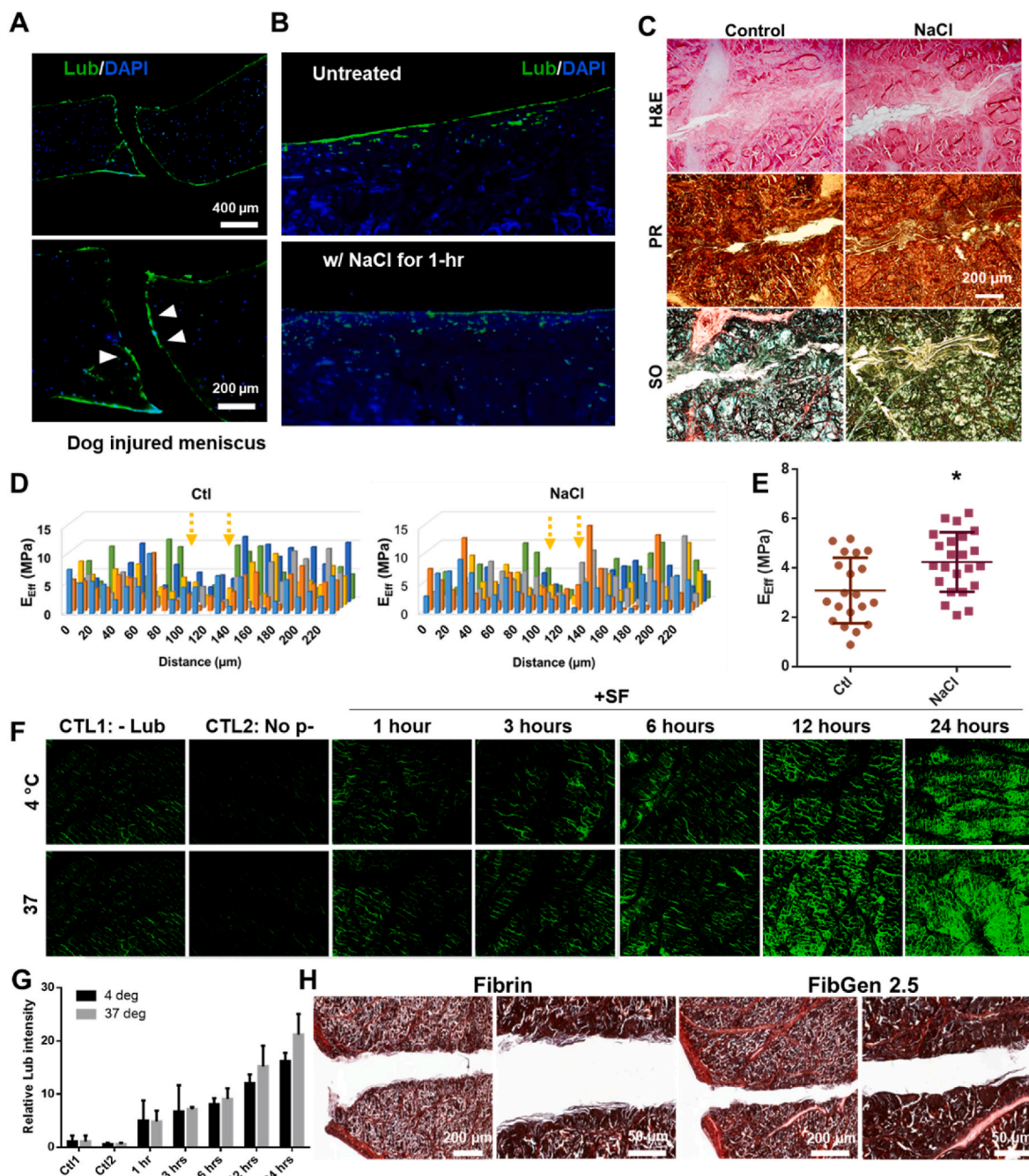

Fig. 3. Untreated, injured dog menisci showed lubricin infiltration on the torn surface (arrow) (A). Treatment with 1 M NaCl for an hour depleted lubricin on the meniscus surface (B) that led to improvement in healing by 4 weeks (C). Nanoindentation-mediated modulus mapping, showing indentation moduli in 220 μm × 120 μm area at 20 μm intervals (D) revealed a modest improvement in healing of NaCl pre-treated explants. Effective modulus (E_{Eff}) from the nanoindentation measurements also showed significant increase in NaCl pre-treated group (E) (*:p < 0.001; n = 25 per group), suggesting an improved functional recovery. Then lubricin coating was established on meniscus explants by incubating with synovial fluids (SF) up to 24 h, resulting in robust lubricin coating on cut surface of bovine menisci as compared to negative controls (no coating and no antibody) (F & G). The lubricin coating for 24 h at 37 °C led to impaired tissue integration and healing both with fibrin and FibGen, delivered with CTGF and TGFβ3-μS (PR staining) (H) (images are from two magnification per group; all samples were lubricin pre-coated).

meniscus healing model. After 4 weeks' culture with syMSCs, lubricin-coated meniscus hardly showed any tissue integration or healing (Fig. 3H). This finding strongly suggest the detrimental effect of lubricin coating on meniscus healing likely by impairing cell and tissue adhesion, consistently with clinical observation [25,35].

2.4. Heparin-conjugated bioactive glue improves healing of lubricin pre-coated meniscus

To improve the initial tissue integration and healing of lubricin-deposited avascular meniscus tears, we devised a strategy to tether lubricin on the torn surface of meniscus. Given the existence of heparin binding domain at N-terminal of lubricin (Fig. 4A), we implemented a heparin-conjugation to our FibGen bio-glue. Heparin conjugation has been applied for controlled delivery of growth factors [36–38] but never been used for tethering lubricin. We synthesized heparin-conjugated fibrinogen by establishing covalent bonding via standard carbodiimide chemistry as shown in Fig. 4B [38]. Briefly, heparin (100 mg) was dissolved in a 0.05 M 2-morpholinoethanesulfonic acid, and 0.04 mM N-hydroxysuccinimide (NHS) and 0.08 mM 1-ethyl-3-(3-dimethylaminopropyl)-carbodiimide hydrochloride (0.08 mM) were applied to activate the carboxylic acid groups of the heparin for 12 h at 48 °C. The solution was then precipitated with excess anhydrous acetone and lyophilized. Then fibrinogen was dissolved in PBS and reacted with activated carboxyl acid groups of the heparin for 4 h. After precipitating with acetone and lypholization, the powder was dissolved in PBS, dialyzed and then lyophilized for 48 h. The prepared heparin-conjugated fibrinogen was used to form fibrin, followed by crosslinking with genipin as per our established methods.

To validate the effect of heparin conjugation, we tested four different bio-glues: (i) fibrin (100 mg/mL fibrinogen and 100 U/mL thrombin), (ii) fibrin crosslinked with 2.5 mg/mL genipin (FibGen), (iii) fibrin mixed with 37.5 mg/mL heparin and 2.5 mg/mL genipin (free Hep-FibGen), (iv) heparin conjugated fibrin crosslinked with 2.5 mg/mL genipin (Conj-Hep-FibGen). Lap shear test with meniscus strips (Fig. 5A) showed that the Conj-Hep-FibGen showed a significant increase in shear modulus as compared to Fib, FibGen, and free Hep-FibGen (Fig. 5B) (n = 8–15 per group; p < 0.0001). Fib-Gen and free Hep-FibGen resulted in marginal increases in the shear modulus as compared to Fib control, as tested with lubricin-coated meniscal tissue strips (Fig. 5B). As compared to the shear strengths tested without lubricin coating, Fib, FibGen, and free Hep-FibGen showed significant decreases when tested with lubricin coated tissues (Fig. 5C). In contrast, conjugated Hep-FibGen led to ~68% increase in shear modulus on lubricin coated tissues (Fig. 5C) (n = 8–15 per group; p < 0.0001). By 4 weeks of explant culture, all the tested bio-glues delivered with CTGF and TGFβ3, including Fib, FibGen, free Hep-FibGen, and conjugated Hep-FibGen, improved tissue integration of avascular meniscus tears through MSC recruitment (Fig. 5D), consistently with our previous works. However, lubricin coating resulted in larger remaining gaps between incised tissues with Fib, FibGen and free Hep-FibGen as compared to control without lubricin coating (Fig. 5D). Only the Conj-Hep-FibGen showed a notable improvement in tissue integration of lubricin-coated avascular meniscus tears as compared to control without lubricin coating (Fig. 5D). Quantitatively, the tensile modulus of healed meniscus was significantly higher with conjugated Hep-Fib-Gen as compared to Fib, Fib-Gen, and free Hep-FibGen (Fig. 5E) (n = 8–15 per group; p < 0.001). Lubricin coating resulted in significant increase in tensile modulus with Conj-Hep-FibGen, whereas Fib, FibGen, and free Hep-FibGen showed significant decreases in tensile modulus (Fig. 5E). Similarly, tensile strength was significantly decreased with lubricin coating in Fib group (Fig. 5F). FibGen and free Hep-FibGen showed marginal increase in tensile strength with lubricin coating as compared to control without coating (Fig. 5F). Conj-Hep-FibGen showed a significantly higher tensile strength with lubricin coating as compared to all the other bio-glue groups (Fig. 5F) (n = 8–15 per group; p < 0.001). These data strongly
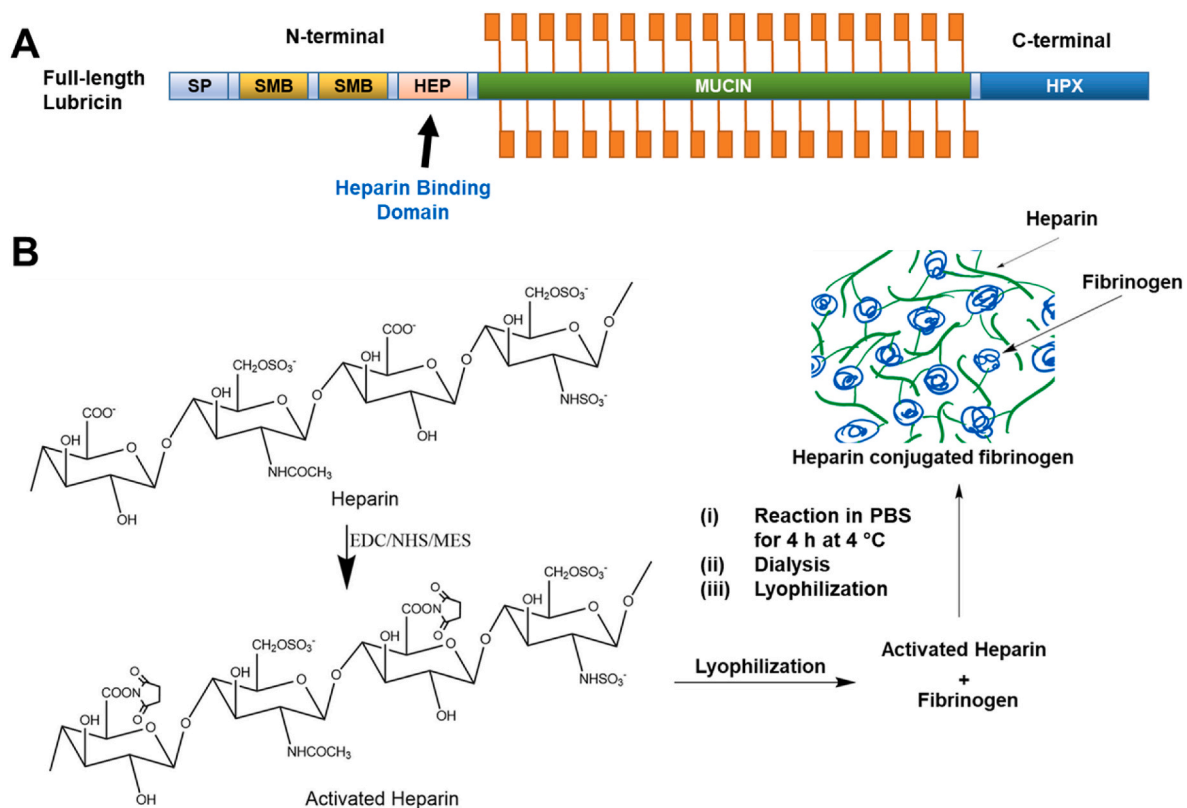

Fig. 4. Heparin-conjugated bio-glue to improve meniscus healing with lubricin infiltration. We target the heparin binding domain (HEP) at N-terminal (A). Heparin-conjugated fibrinogen was synthesized by establishing covalent bonding via standard carbodiimide chemistry (B).
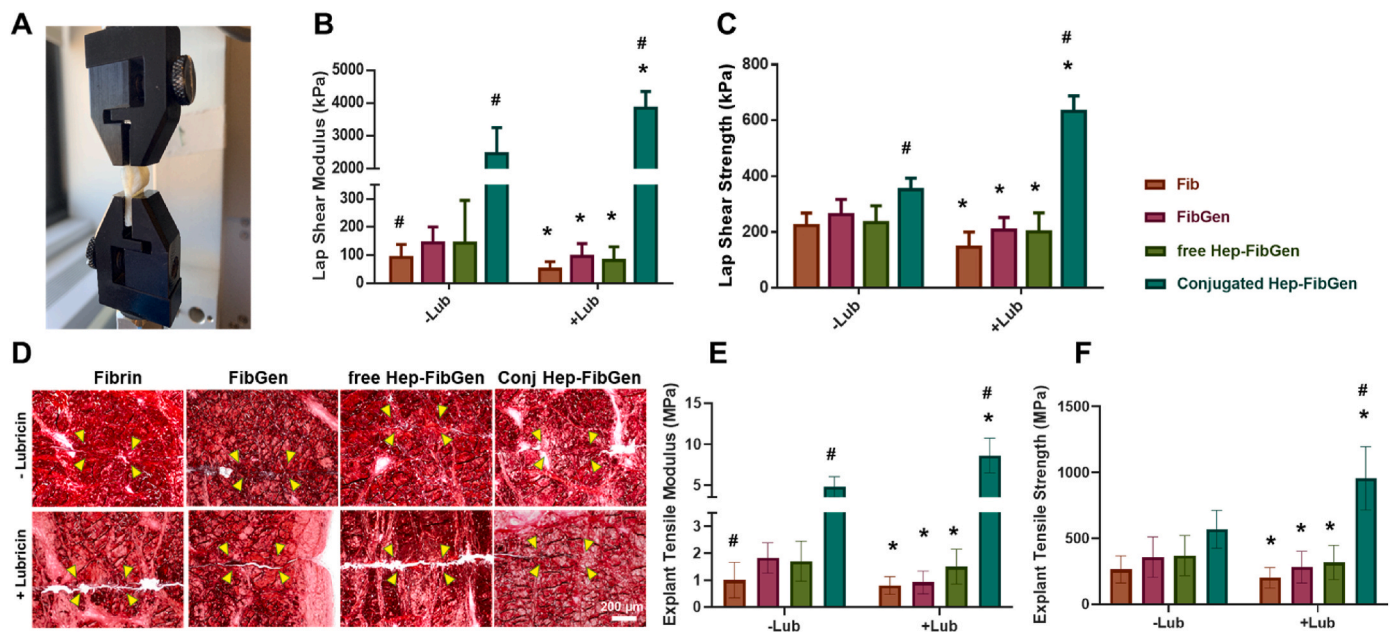
Fig. 5. Lap shear tests of different bio-glues were conducted with lubricin-coated meniscus tissue strips (A). Lap hear modulus (B) and lap shear strength (C) significantly increased by heparin-conjugated FibGen with lubricin coating compared to no coated control (n = 8–15 per group; *p < 0.001 compared to no-coating control; #:p < 0.001 compared to all the other groups). Histology with PR staining showed the good tissue integration of lubricin-precoated meniscus tears with Heparin-conjugated FibGen (D). Consistently, tensile modulus and strength were significantly increased by heparin-conjugated FibGen (E, F) (n = 8–15 per group; *p < 0.001 compared to no-coating control; #:p < 0.001 compared to all the other groups).

suggest the efficiency of heparin conjugation on promoting initial tissue bonding and healing of meniscus tears pre-deposited with lubricin.

2.5. Matrix components involved with lubricin binding on torn meniscus surface

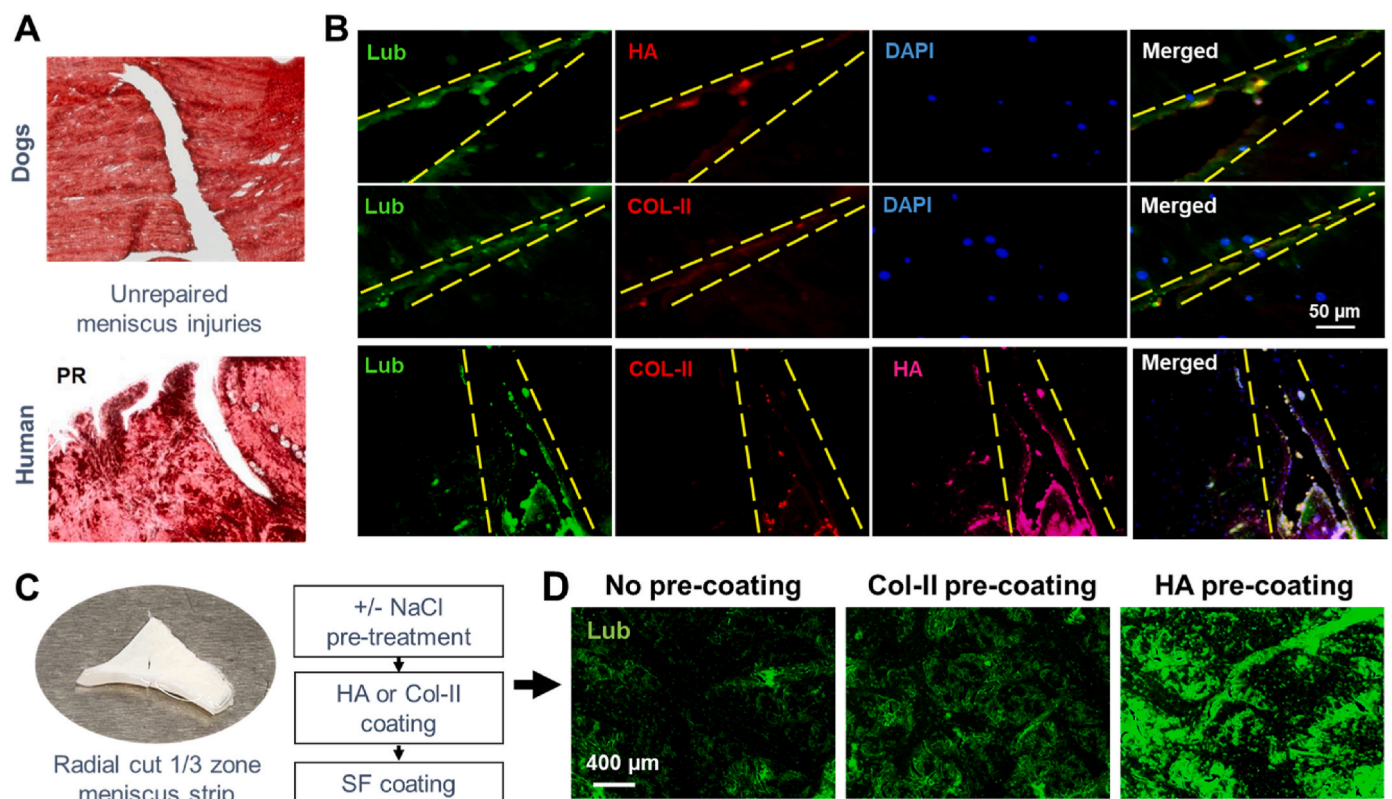To understand how lubricin is deposited and coated on the torn

Fig. 6. Injured menisci from dog and human (A) showed lubricin expression on torn surface, largely co-localized with HA and some of COL-II (B). Consistently, radially cut meniscus strips (C) showed a higher binding of lubricin on the HA pre-coated surface as compared to COL-II pre-coating and no pre-coating (D).

surface of menisci, we performed immunofluorescence labeling with multiple matrix proteins expressed in joint tissues. The lubricin expression on torn surface of unrepaired, injured dog and human menisci (Fig. 6A) was largely co-localized with HA (Fig. 6B). COL-II was also partially co-localized with lubricin expression both on dog and human injured menisci (Fig. 6B). Lubricin expression on the articular surface of healthy human meniscus with no injury was also co-localized with HA and COL-II, similarly with degenerating human meniscus (Suppl. Fig. 3). To confirm the role of HA and COL-II on lubricin binding on torn meniscus surface, we treated radially cut meniscus explants with NaCl to remove any lubricin residue which were then pre-coated with HA or COL-II for an hour, following by washing with PBS and incubation in SF for an hour (Fig. 6C). There was abundantly more lubricin deposition on the HA pre-coated tissue surface as compared to samples without pre-coating (Fig. 6D). Pre-coating with COL-II also showed a modest increase in the lubricin deposition (Fig. 6D). These findings suggest that HA and/or COL-II pre-deposition precede the lubricin deposition on the tear surface of meniscus, likely consistent with previous findings suggesting roles of HA and COL-II on binding of lubricin articular surface [23,39].

2.6. Incorporation of CD44 to further strengthen the tethering through lubricin and HA

Given the pivotal role of HA in the lubricin deposition and retention on torn meniscus surface (Fig. 6), we adopted CD44 into our bioactive glue to further strengthen the initial bonding. CD44 is a transmembrane glycoprotein present in many different types of cells including synovial MSCs [29] that shows a strong binding affinity to lubricin as well as HA [29,40]. CD44 can be readily prepared as incorporated in FibGen given

the well-described binding mechanism between CD44 and fibrin(ogen) through O- & N-linked glycosylation [41,42] (Fig. 7A). Given the CD44's HA-binding motif (BX7B) likely distinct to its lubricin-binding site [41] (Fig. 7A), we hypothesized that incorporation of CD44 in our FibGen glue will further strengthen the tissue bonding by providing tethering with lubricin and HA (Fig. 7B). To first confirm the CD44's binding to lubricin, we applied 5 µg/mL of CD44 [42] on lubricin-rich articular surface of bovine meniscus that resulted in abundant coating of CD44 on lubricin$^+$ surface (Fig. 7B). However, when surface lubricin was depleted by 1 M NaCl treatment, CD44 was hardly bound on the meniscus surface (Fig. 7B).

To measure the binding force between CD44 and the proteins of interest, we established a quantitative measurement method using PIUMA™ nano-indenter (Optics11, Amsterdam, The Netherlands). The probe tip (with 0.2–0.6 N/m stiffness and 45–60 µm tip radius) of the nano-indenter was functionalized by CD44 as per the manufacturer protocol and previously published procedure [43] (Fig. 7C). Briefly, the probe was brought down by controlling the microstepper motors to immerse the tip into the protein G (10 µg/mL) droplet on a glass slide for 5 min. The probe tip was air dried for 30 min after removing the excess solution by briefly dipping the probe in the solution. Then CD44 Fc chimera protein (10 µg/mL, R&D, Minneapolis, MN) was coated, followed by crosslinking between protein G and CD44 using bis(sulfosuccinimidyl) suberate (50 mM BS3, Thermo Fisher Scientific, Waltham, MA). Finally, CD44 coated probe tip was washed three times with DI water for 2 min each time. Then a series of indentations were performed under a maximum force of 10 mN and 20 µm step size on the hydrogels for adhesion force measurement between CD44 and fibrin, HA, COL-I, COL-II, and lubricin overcoating on those hydrogels (Fig. 7C). All indentation measurements were performed in PBS at room temperature.
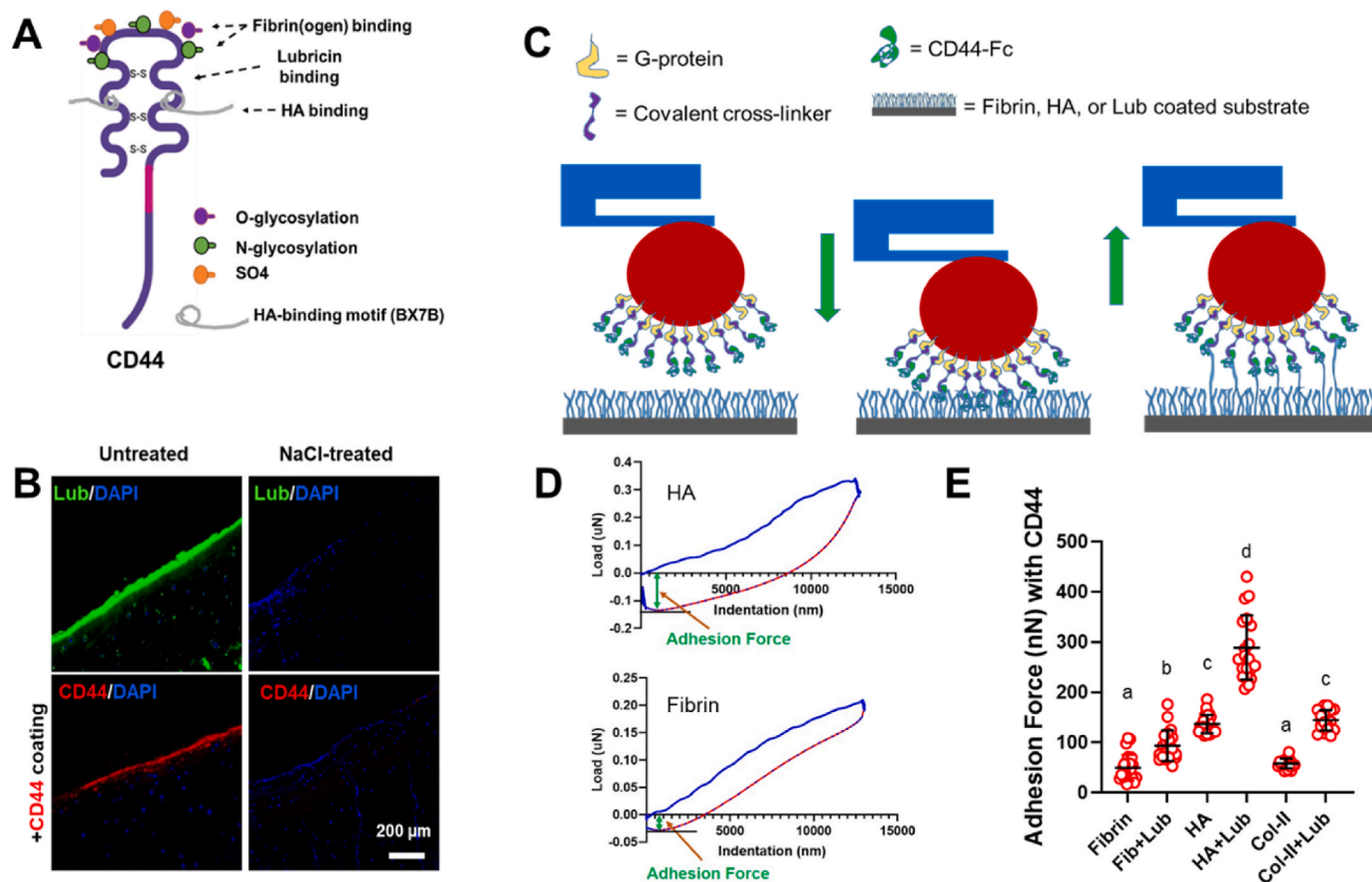

Fig. 7. CD44, a transmembrane glycoprotein, has a reported binding affinity to HA, lubricin, and fibrin(ogen) (A). CD44 readily bound on the articular surface of meniscus where lubricin was present, but not on NaCl-treated surface with depleted lubricin (B).

Adhesion force was determined from the maximum deflection from baseline in the force vs displacement output retraction curve (Fig. 7D). As result, CD44 showed the higher binding force to HA as compared to fibrin and COL-II (Fig. 7D). Lubricin overcoating on fibrin, COL-II, and HA layer significantly increased binding force to CD44 (Fig. 7D). Among all the tested groups, CD44 showed the highest binding force to HA and lubricin double coating (Fig. 7D) (p < 0.0001; n = 25 per group), suggesting the potential of CD44 for integrating meniscal tissues by tethering HA and lubricin.

Heparin conjugated FibGen with CD44 as an advanced bioactive glue facilitating healing of HA/lubricin-coated meniscus injuries.

Given the strong binding affinity of CD44 with HA and lubricin, we prepared CD44 incorporated, heparin conjugated FibGen (Hep-FibGen) (Fig. 8A) and tested its functionality for meniscus integration and healing. On lubricin-coated meniscal tissues, incorporation of CD44 in Hep-FibGen showed no statistically significant improvement in the lap shear modulus and strength as compared to Hep-FibGen without CD44 (Fig. 8B) (p < 0.001; n = 8 per group). On HA/lubricin-coated meniscus surface, CD44 incorporation resulted in significant improvements in the

lap shear modulus and strength (Fig. 8C) (p < 0.001; n = 8 per group). When applied for our well-established meniscus explant injury healing model with CTGF and TGFβ3-μS delivery, both FibGen-CD44 and Hep-FibGen-CD44 resulted in promising tissue integration and healing by 6 weeks as compared to FibGen with some remaining tissue gap (Fig. 8D). FibGen-CD44 and Hep-FibGen-CD44 showed ~1.8 and ~2.7-fold increases in the tensile modulus and strength, respectively, compared to FibGen (Fig. 8E) (p < 0.001; n = 8 per group). Hep-FibGen-CD44 showed significantly higher increases in the tensile properties than FibGen-CD44 (Fig. 8E), suggesting the combinational effect of heparin conjugation and CD44 incorporation. Modulus mapping with nanoindentation showed no significant differences between FibGen, FibGen-CD44, and Hep-FibGen-CD44 (Suppl. Fig. 4).

3. Discussion

Lubricin is a surface-active mucinous glycoprotein, an essential component of synovial joints playing an irreplaceable role in providing near frictionless joint motion [21]. As referred to as superficial zone
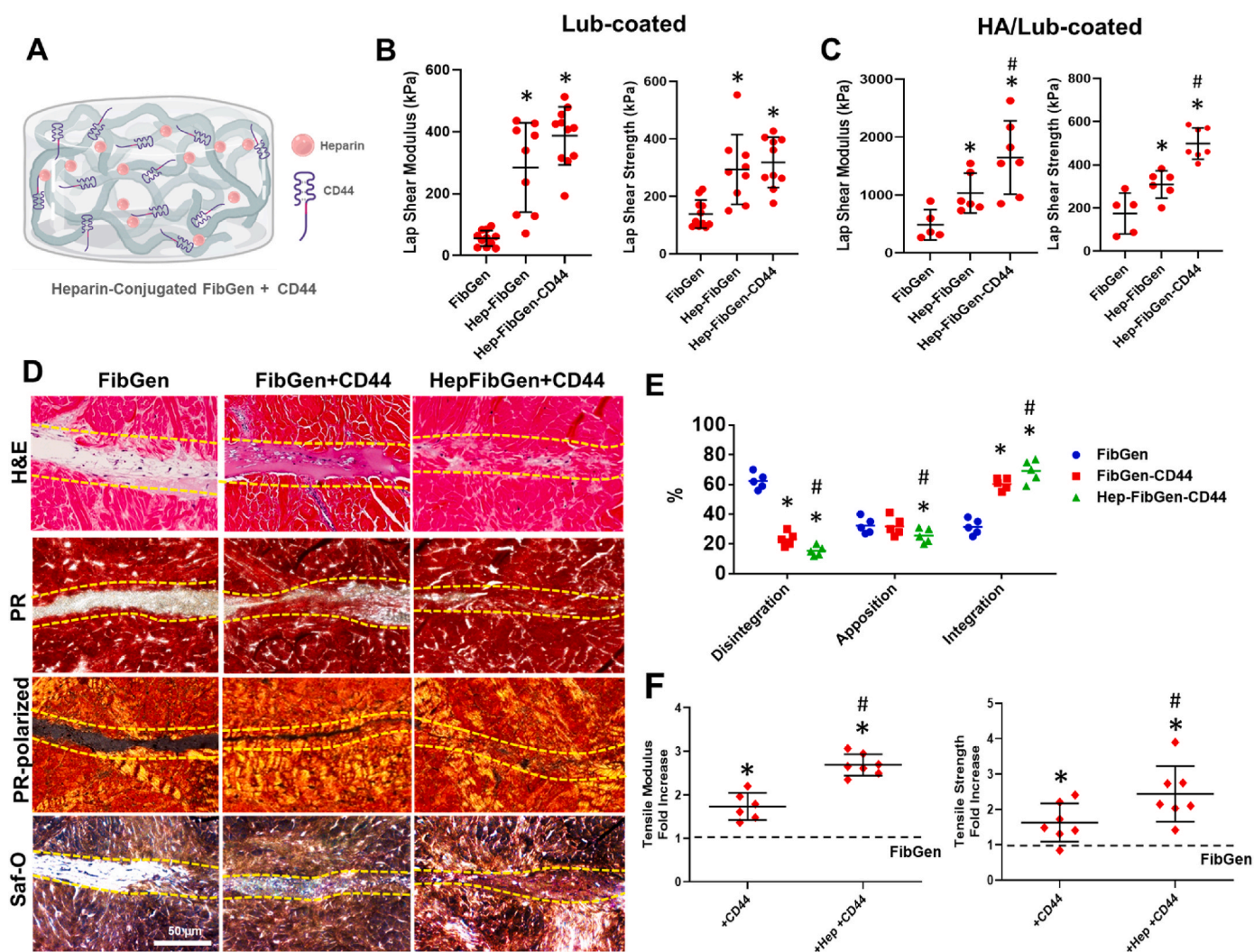

Fig. 8. Heparin conjugated FibGen incorporated with CD44 (Hep-FibGen-CD44) (A) showed significantly higher lap shear modulus and strength compared to FibGen on lubricin-coated meniscal tissues, with no significant difference from FibGen-CD44 (B) (*:p < 0.001; n = 10 per group). In contrast, Hep-FibGen-CD44 showed significantly higher lap shear and modulus as compared to Hep-FibGen on HA/lubricin-coated meniscal tissues (C) (*:p < 0.001 compared to FibGen, #:p < 0.001 compared to Hep-FibGen; n = 10 per group). Histologically, delivery of CTGF and TGFβ3-μS via Hep-FibGen-CD44 and Hep-FibGen improved the healing of avascular meniscus tears as compared to FibGen (D) (dash-line: healing zone). Quantitative histomorphometry measurements show significant improvement of tissue integration with FibGen-CD44 and Hep-FibGen-CD44 (E) (*:p < 0.001 compared to FibGen, #:p < 0.001 compared to FibGen-CD44; n = 5 per group). By 6 weeks, the tensile modulus and strength (F) of healed meniscus were significantly higher with CD44 incorporation and heparin conjugation than FibGen (*:p < 0.001 compared to FibGen, #:p < 0.001 compared to FibGen-CD44; n = 6–7 per group).

protein (SZP), lubricin is predominantly expressed by the cells at the superficial zone of articular cartilage and meniscus [21]. Given its unique function and spatial expression pattern, the roles of lubricin in protecting joint tissues from degenerative changes in osteoarthritis have been widely investigated [22–24,28,30,31]. Previous studies reported that depletion of lubricin further accelerates cartilage damage while over-expression of lubricin prohibits the progression of osteoarthritis [28,30,31]. Lubricin expression has also been a focus in the tissue engineering of joint tissues [23]. In contrast, this study suggested lubricin's new, detrimental role in tissue healing, likely derived from its unique functions preventing cell and tissue adhesion that enables near-frictionless joint movements. As torn menisci are exposed to lubricin-rich synovial fluid until being surgically treated days to weeks after the injury, lubricin inevitably infiltrates into the torn surface. We confirmed consistent lubricin deposition on torn surfaces of injured menisci from dogs and human patients. These new observations realized the importance of lubricin for developing a clinically applicable bioengineering approach to facilitate functional healing of meniscus injuries. In addition, our observations may advocate for the necessity to consider lubricin for regenerative approaches for other intra-synovial tissues such as intra-articular tendons and ligaments.

Our first approach to address the harmful effects of lubricin deposition on torn meniscus surfaces was a chemical modification to our bioactive glue to add tethering through pre-coated lubricin. We adopted heparin-conjugated fibrinogen to achieve this goal given the existence of the heparin-binding domain (HEP) at the N-terminal of lubricin [21,28]. As fully extended lubricin monomers/dimers bind to the articular cartilage via the C-terminal [21,22,24], we hypothesized that binding through HEP at the N-terminal provides additional adhesion force. As demonstrated by our data, heparin conjugation in our bioactive glue significantly improved the initial bonding strength and integrated healing of lubricin-coated menisci. Previously, heparin-conjugated fibrin was used to enhance the efficacy of fibrin gel as a drug delivery carrier [36–38]. Heparin-conjugated fibrin shows a prolonged release of various growth factors by providing binding sites for the proteins [36–38]. Since no previous study has implemented heparin-conjugation for tethering lubricin or enhancing the physical properties of the hydrogel, our approach represents a novel application of heparin-conjugation in fibrin-based hydrogel.

Interestingly, heparin conjugation not only added binding affinity to lubricin but also further increased the mechanical properties of FibGen hydrogel. Genipin crosslinking happens through ring opening attacked by amine groups, followed by covalent bonding and re-closure of rings. As both fibrin and heparin have an amine group, pre-conjugation with heparin likely resulted in additional crosslinks leading to improved mechanical properties. Thus, we speculate that the refined controls of heparin conjugation and genipin crosslinking would be necessary to avoid excessive crosslinking resulting in a highly dense matrix that was unsuitable for tissue ingrowth. The ratio of heparin to fibrin and genipin pre-optimized in this study appeared to be effective for increasing mechanical properties and lubricin-binding affinity without interfering with the biocompatibility of bioactive glue. However, those concentrations and ratios may need to be re-visited for *in vivo* studies in consideration of the species, size, and metabolism of the preclinical animal model chosen.

One of the interesting findings from the previous studies on lubricin is that lubricin readily binds to the articular surface of cartilage but not the deep cartilage zone [22,24]. Follow-up studies suggested that lubricin binding on the articular surface is mediated by other matrix proteins, including HA, COL-II, and cartilage oligomeric matrix protein (COMP), that are abundant on the superficial zone [22,39,44]. Our *in vitro* experiment confirmed that pre-coating with HA is likely necessary for the proper binding of lubricin on the torn surface of the deep meniscus zone. However, the timing for HA and lubricin to deposit on the torn surface is still unknown. In addition, because HA is predominantly produced by superficial zone cells [45], it is still unclear if deep

zone meniscal cells may produce HA upon contact with synovial fluid or HA is sourced from synovial fluid. Unfortunately, it is very difficult to obtain tissues from torn menisci within days to weeks of injury such that the canine and human torn meniscus tissues available for this study had months-old injuries. Thus, follow-up studies with conditional HA knockout mouse models [46] may be necessary to answer those questions.

Nonetheless, the revealing of HA pre-deposition leading to lubricin deposition on torn meniscus surfaces led us to an additional intervention using CD44 to enhance the tissue integration further. CD44 is a surface receptor expressed in various cells, including synovial MSCs, with a strong binding affinity to lubricin and HA [29]. As CD44 forms strong binding to fibrin(ogen) via a specific binding site, CD44 incorporation into Hep-FibGen significantly enhanced the initial bonding and integrated healing of HA/lubricin-coated meniscal tissues. As a surface receptor, binding of CD44 with lubricin may be involved with various intracellular signaling associated with inflammatory responses [40]. However, we used recombinant CD44 as a separate matrix component outside cell for providing tethering with HA and lubricin, without a concern of causing undesired biological activities. We speculate that CD44 and heparin provide a synergistic effect on binding to torn meniscus through multiplexed interactions between CD44, heparin, HA, and lubricin, as depicted in Fig. 9. One of the remaining questions is whether CD44 shares its binding motifs for HA, fibrin(ogen), and lubricin. If CD44 binding is competitive among these three types of matrix proteins, it would be technically challenging to quantitatively evaluate the effects of CD44 incorporation on meniscus integration and healing. However, our quantitative measurement using nanoindentation suggested that CD44 binding is not competitive among these matrix proteins by showing a significantly higher binding affinity on HA/lubricin-coated substrates.

The limitations of this study include the complexity of bioactive glue containing multiple factors such as FibGen, heparin, and CD44, which
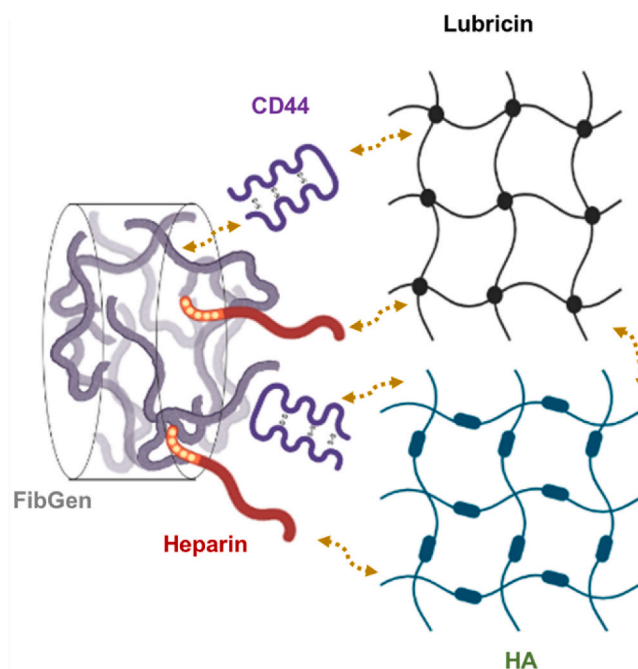
Fig. 9. Speculated mechanism for synergistic effect of heparin conjugation and CD44 incorporation on yielding strong binding to HA- and lubricin-coated meniscus surface. Although specific binding domain, mechanism, and affinity between each other components have been incompletely described, the cross-binding affinity between HA, lubricin, fibrinogen, heparin, and CD44 may have potential to achieve a strong initial binding of our bioactive glue on HA/lubricin-deposited meniscus surface.

may serve as a translational barrier. Nonetheless, our heparin-conjugated FibGen with CD44 can be produced as a ready-to-use package like the clinically available fibrin sealants that would not include any unnecessary operational difficulties for surgeons. The foreseeable translational step will include a reduction process to simplify the final product by replacing the major components with alternative chemical compounds. Another limitation of this study is the lack of *in vivo* tests. Although our previous study demonstrated the fibrin-based glue delivered with CTGF and TGFβ3 μS successfully guided integrated healing of avascular meniscus tears in rabbits [9], the *in vivo* efficacy of the present bioactive glue in lubricin-infiltrated, untreated meniscus injuries has not been validated *in vivo*. To validate the roles of HA/Col-II on lubricin deposition after injury and detrimental effect of lubricin infiltration into the torn surface, we may consider mouse models with conditional HA or Col-II knockout. However, the surgery for meniscus injury and repair is not feasible in such a small animal model. Use of large animal models is limited by the high cost. Accordingly, we focused on *ex vivo* models to perform the proof-of-concept study for the newly devised bioactive glues addressing the harmful effect of lubricin infiltration into meniscus injuries. Future studies will explore the *in vivo* efficacy of our bioactive glue in clinically relevant animal models with untreated meniscus injuries.

To conclude, this study suggests a novel and effective approach to promote the healing of avascular meniscus tears using advanced bioactive glue, providing a strong bonding to HA/lubricin-coated torn meniscus surface and guiding regenerative healing via stem/progenitor cells recruitment. In addition, our study identified a novel application of heparin conjugation and CD44 as an effective tool to support the binding of HA/lubricin-deposited tissue surface. Our bioactive glue with heparin conjugation and CD44 incorporation may be effective for healing other intra-articular tissues such as flexor tendons, rotator cuffs, cruciate ligaments, and temporomandibular joint (TMJ) disc.

4. Methods

4.1. Preparation of FibGen, Hep-FibGen, and Hep-FibGen-CD44

FibGen was prepared by mixing an equal volume of 200 mg/mL fibrinogen (MW: 340 kDa; Sigma-Aldrich, St. Louis, MO) with 200 U/mL thrombin (40–300 NIH units/mg protein; Sigma-Aldrich, St. Louis, MO) with 2.5 mg/mL (final concentration) of genipin (≥98% HPLC; Sigma-Aldrich, St. Louis, MD) mixed with thrombin. Heparin-conjugated fibrinogen was synthesized by establishing covalent bonding via standard carbodiimide chemistry as per previous methods [38]. Briefly, heparin (200 mg) was dissolved in DI water, and 0.04 mM N-hydroxysuccinimide (NHS) and 0.08 mM 1-ethyl-3-(3-dimethylaminopropyl)--carbodiimide hydrochloride (EDAC) were applied and kept for 12 h at 4 °C to activate the carboxylic acid groups of the heparin. Fibrinogen solution (100 mg in 20 mL phosphate-buffered saline (PBS)) was then added to the above heparin solution and kept at 4 °C for 3 h to complete the reaction with the activated carboxyl acid groups of the heparin. This heparin-conjugated fibrinogen solution was then dialyzed against DI water through a semi-permeable membrane (12,000–14,000 Da molecular weight cutoff; Sigma) at 4 °C for 48 h with changing the DI water every 12 h. Finally, heparin-conjugated fibrinogen powder was collected after lyophilization for 48 h. The prepared heparin-conjugated fibrinogen was used to form fibrin by mixing heparin-conjugated fibrinogen (200 mg/mL) and thrombin (200 U/mL), followed by crosslinking with genipin as described above. As a comparison group, free heparin fibrinogen was prepared by simply mixing fibrinogen (200 mg/mL) in heparin (200 mg/mL) in PBS. To prepare CD44-incorporated hydrogels, CD44 (5 μg/mL; R&D Systems, Minneapolis, MN) was mixed with thrombin using repeated pipetting before preparing the bioactive glue. Our pilot experiment confirmed the even distribution of CD44 in fibrin using image-based analysis (data not shown). The prepared solution of fibrinogen (w/heparin±CD44) and thrombin/genipin were co-injected

in between the incised tissue surfaces using FibriJet® dual-injector with a blending applicator (Nordson Micromedics, Westlake, OH).

4.2. Meniscus explant for avascular healing by MSCs recruitment

A meniscus explant model was used to study *in vitro* healing of avascular meniscus tears. Menisci were isolated from skeletally mature (18–24 months old) bovine knee joints obtained from Animal Technologies, Inc (Tyler, TX). The isolated menisci were rinsed twice with 10X antibiotics (100 units/mL of penicillin & 100 μg/mL of streptomycin), twice with 1X antibiotics 10 units/mL of penicillin & 10 μg/mL of streptomycin), and then washed in PBS, with each washing step for 5 min. The inner third zone of the menisci were cut and prepared as wedge-shaped tissue explants in a thickness of 2–3 mm. Then full-thickness longitudinal incisions were made in the middle of the inner third zone, and prepared bioactive glues loaded with 1000 ng/mL CTGF (BioVendor, Asheville, NC) and 10 mg/mL PLGA μS-encapsulating TGFβ3 (R&D systems) (2.5 μg per 500 mg PLGA) was applied to the incised tissues. Then the meniscus explants were placed on top of monolayer-cultured P2 – P3 syMSCs or hBMSCs (AllCells, Alameda, CA) at 80–90% confluence per our previous methods [8,9]. Supplements for fibrogenic and chondrogenic differentiation were applied as described in our recent publication [8,9]. By 4–6 weeks, tissue healing and integration were evaluated using histology with H&E, Picrosirius Red (PR)/polarized microscopy, and Safranin O (Saf-O) as per our prior methods [47–50].

4.3. Preparation of TGFβ3 encapsulated in PLGA microspheres

PLGA (66,000–107,000 Mw) with a PLA/PGA ratio of 75:25 was purchased from Sigma-Aldrich (St. Louis, MO). PLGA μS encapsulating recombinant human TGFβ3 were prepared by a modified double-emulsion technique [49,51], a well-established control-delivery vehicle demonstrating preserved bioactivity of growth factors. Briefly, 500 mg PLGA was dissolved into 5 mL chloroform, followed by adding 250 μL of diluted TGFβ3. This solution was then emulsified (primary emulsion) by ultrasonication for 5 min to reduce the size of μS(52). The primary emulsion (w/o) was then added to 10 mL 4% (w/v) PVA (poly vinyl alcohol) solution to form the second emulsion (w/o/w) by 2 min of ultrasonication followed by 1-min vortexing. This double emulsion solution was then added to 250 mL of 0.3% PVA solution, followed by continuous stirring for 2 h to evaporate the solvent. Finally, the μS were filtered, washed with DI water, resuspended in DI water, and then lyophilized. Release kinetics of TGFβ3 was reported in our previous studies [49,50].

4.4. Release kinetics of CTGF

For release rate measurement, CTGF-loaded (30 ng/mL) fibrin and FibGen gel mixed with CTGF were incubated at 37 °C with gentle agitation for 6 wks in PBS. Equal volume of fibrinogen (50 mg/mL) and thrombin (50 U/mL) was mixed to make fibrin and fibgen gels. The concentration of genipin in the FibGen was 2.5 mg/mL. At selected time points, incubation media was collected and concentration of CTGF was measured using ELISA as per our previous works [9,50].

4.5. Lap shear test

Strips of bovine menisci will be cut into 40 × 4 mm dimensions for the lap shear test. 20 μL bio-glue was applied in between the bovine meniscus tissue strips. The adhered strips were mounted by tensile jigs in BioDynamics testing system (TA instruments, New castle, DE), followed by applying displacement at 0.02 mm/s. From load-displacement curves, lap shear modulus and strength were obtained.

4.6. Blot migration assay

To measure the migration of syMSCs, 100 μL of fibrin- or FibGen-loaded with 1000 ng/mL CTGF were applied on one side of 6 well culture plates, followed by 30-mins incubation for crosslinking. Then CFDA-labeled syMSCs were plated on the other side of the culture well. Up to 48 h, the number of migrating cells toward the hydrogel was counted using fluorescence microscopy and quantified. To test the role of CD44 in CTGF-induced cell migration, we blocked the CD44 by applying 5 μg/mL neutralizing antibody (#103012, BioLegend, San Diego, CA) and repeated the migration assay above.

4.7. In vitro degradation assay

Fibrin and FibGen with 2.5 mg/mL – 10 mg/mL genipin were prepared as described above. The 30 μL of each hydrogel was incubated at 37 °C in PBS, and then the fibrin degradation products were measured using ELISA for up to 21 days with a commercial kit (Novus Biologicals, LLC, Centennial, CO).

4.8. Tensile tests

Following a well-established testing protocol for meniscus explants[19], samples for the tensile tests were prepared as 8 mm in length, 2 mm in width, and 1 mm in thickness, as modified from our prior works [9,33,49]. Upon mounting with tensile jigs in an isotonic saline bath at RT, a 0.02-N tare load will be applied to the samples, and then the samples will be elongated at 10%/min until failure. From the force vs. elongation curve, the ultimate strength and tensile modulus were obtained. All pull-out tests were performed using BioDynamics testing system.

4.9. Modulus mapping and surface congruency

Nanoindentation experiments were conducted using a PIUMA™ nano-indenter (Optics11, Amsterdam, The Netherlands) with a probe tip diameter of 8–10 μm with the sample loaded to a maximum force of 10 mN. All nanoindentation tests were carried out on fixed and unstained tissue sections [53]. A series of indentations were performed to determine the effective indentation modulus (E_{Eff}) across a healed region at every 20 μm distance from the original defect site, using the embedded high-precision mobile X–Y stage.

4.10. Nanoindentation-based binding force measurement

Adhesion force measurement was performed using PIUMA™ nano-indenter. The probe tip (with 0.2–0.6 N/m stiffness and 45–60 μm tip radius) of the nano-indenter was functionalized by CD44 as per the manufacturer protocol and previously published procedure [43]. Briefly, for protein G coating, the probe was brought down by controlling the microstepper motors directly from the PIUMA software so that only the probe tip gets immersed into the protein G (10 μg/mL) droplet on a glass slide for 5 min. The probe tip was air-dried for 30 min after removing the excess solution by briefly dipping the probe in the protein G solution. Similarly, CD44 Fc chimera protein (10 μg/mL, R&D Systems, Minneapolis, MN) was coated, followed by crosslinking between protein G and CD44 using bis(sulfosuccinimidyl) suberate (50 mM BS3, Thermo Fisher Scientific, Waltham, MA). Finally, CD44 coated probe tip was washed three times with DI water for 2 min each time. Then a series of indentations were performed under a maximum force of 10 mN and 20 μm step size on the hydrogels for adhesion force measurement between CD44 and fibrin (a mixture of 100 mg/mL fibrinogen and 100 U/mL thrombin, HA (hyaluronic acid) (2% methacrylated HA, Mw 50, 000–70,000), type I collagen (2.5 mg/mL) and type II collagen (2 mg/mL) gels w/o lubricin (2 μg/mL) (MyBiosource, San Diego, CA) overcoating on those hydrogels. The hydrogel coating was applied on the surface of the tissue culture plate by applying an un-crosslinked hydrogel solution, followed by incubation for an hour for crosslinking. Double coating, we first coated the first hydrogel (fibrin, HA, and COL-II), crosslinked for an hour, washed away the residue solution, and then applied the second coating protein (e.g., lubricin). All hydrogels were purchased from Sigma (St. Louis, M O) except type I collagen (ThermoFisher Scientific, Waltham, MA). Hydrogels were incubated with lubricin solution for 30 min at room temperature for lubricin coating, followed by washing with DI water three times. All indentation measurements were performed under PBS at room temperature. Adhesion force was determined from the maximum deflection from baseline in the force vs displacement output retraction curve.

4.11. Dog and human meniscus samples

Injured medial and lateral menisci were recovered from skeletally mature purpose-bred female hound-mix dogs (n = 3) humanely euthanized at the University of Missouri Thompson Laboratory for Regenerative Orthopaedics following completion of an IACUC-approved study performed for reasons unrelated to the present study. The menisci underwent arthroscopically-assisted creation of 5 mm longitudinal tears in the red-white zone of each meniscus 3 months prior to recovery.

With IRB-approval and documented informed consent, injured human medial menisci were obtained from patients (n = 2; 51 yM, 59 yF) undergoing open knee surgery for symptomatic post-traumatic osteoarthritis with pre-operatively diagnosed chronic meniscal tears. With IRB approval and documented donor family consent for research use, intact medial and lateral menisci were recovered from healthy human tissue donors (n = 2; 21 yM, 33 yF) as non-implanted tissues that would otherwise be discarded after osteochondral and/or meniscus allograft transplantation surgeries. Meniscus tissues were delivered to Columbia University for histological analysis without disclosure of any identifying patient or donor information.

4.12. Immunofluorescence

Following our prior methods [50,52,54], immunofluorescence was performed to image tissue sections using monoclonal antibodies and isotype-matched Alexa Fluor® secondary antibodies, with nucleus labeling with DAPI. All the tissue sections were made in 5-μm thickness, and the antigen retrieval procedures were performed following the manufacturer's protocols. CD44 (3660-CD-050, R&D Systems), lubricin (aa1151-1241, LSBio, Seattle WA), hyaluronic acid methacrylate (914800, SigmaAldrich), and/or type II collagen (COL-II) (C9301, Sigma-Aldrich) were co-labeled with multiple fluorescent secondary antibodies to track recruitment and differentiation of endogenous syMSCs. All primary antibodies and secondary antibodies were purchased from Abcam (Cambridge, MA), Santa Cruz Biotechnology (Dallas, Texas) or Life Technologies (Grand Island, NY). All images were acquired using an inverted fluorescence microscope (Olympus IX73, Waltham, MA).

4.13. Histomorphometry analysis

The quality of meniscus tissue repair was evaluated using a modified quantitative histomorphometry measurement [34]. Briefly, % of disintegration, unbound interface with no apposition or bonding between meniscal tissues, was calculated as the length of disintegrated interface in μm divided by total length of healing interface, multiplied by 100 (%). Similarly, % of apposition was calculated for the length of issue interface joined and continuous but with no clear sign of matrix remodeling. In addition, % of integration was calculated for the length of interface with fully bonded and matrix remodeling. To ensure unbiased data acquisition, three blinded examiners evaluated the tissue section slides.

4.14. Statistical analysis

For all the quantitative data, following confirmation of normal data distribution, one-way analysis of variance (ANOVA) with post-hoc Tukey HSD tests was used with p-value of 0.05. Sample sizes for all quantitative data were determined by power analysis with one-way ANOVA using a level of 0.05, power of 0.8, and effect size of 1.50 chosen to assess matrix synthesis, gene expressions, and mechanical properties in the regenerated meniscus tissues and controls upon verification of normal data distribution.

Ethics approval and consent to participate

Not applicable; no animal; no human subjects.

CRediT authorship contribution statement

Solaiman Tarafder: was responsible for the primary technical undertaking and conducted the experiments. **Jaskirti Ghataure:** performed the experiments for genipin crosslinking of fibrin. **David Langford:** performed the experiments for genipin crosslinking of fibrin. **Rachel Brooke:** performed the heparin-conjugation experiments. **Ryunhyung Kim:** assisted in the experiment for meniscus explant healing and lap shear tests. **Samantha Lewis Eyen:** assisted the nano-indentation measurements and analysis. **Julian Bensadoun:** assisted in the experiments for lubricin deposition and binding through matrix components. **Jeffrey T. Felix:** assisted in the experiments for lubricin deposition and binding through matrix components. **James L. Cook:** participated in the overall study design and provided injured meniscus tissue samples from dog and human patients. **Chang H. Lee:** is responsible for the study design, Formal analysis, and interpretation, and manuscript preparation, All the authors edited the manuscript.

Declaration of competing interest

The authors declare that they have no known competing financial interests or personal relationships that could have appeared to influence the work reported in this paper.

Acknowledgements

Appendix A. Supplementary data

Supplementary data to this article can be found online at https://doi.org/10.1016/j.bioactmat.2023.04.026.

References

[1] C.D.C. Center, For Disease Control and Prevention Report, 2011.
[2] J.L. Cook, D.B. Fox, A novel bioabsorbable conduit augments healing of avascular meniscal tears in a dog model, Am. J. Sports Med. 35 (11) (2007) 1877–1887.
[3] K.A. Athanasiou, J. Sanchez-Adams, in: J.K. Kent Leach (Ed.), Engineering the Knee Meniscus. Athanasiou KA, Morgan and Claypool Publishers, 2009 March 30, p. 2009.
[4] B.M. Baker, A.O. Gee, N.P. Sheth, G.R. Huffman, B.J. Sennett, T.P. Schaer, et al., Meniscus tissue engineering on the nanoscale: from basic principles to clinical application, J. Knee Surg. 22 (1) (2009) 45–59.
[5] F.R. Noyes, S.D. Barber-Westin, Repair of complex and avascular meniscal tears and meniscal transplantation, J Bone Joint Surg Am 92 (4) (2010) 1012–1029.
[6] J.M. Patel, A. Brzezinski, D.A. Raole, M.G. Dunn, C.J. Gatt Jr., Interference screw versus suture endobutton fixation of a fiber-reinforced meniscus replacement device in a human cadaveric knee model, Am. J. Sports Med. 46 (9) (2018) 2133–2141.
[7] F. Qu, M.P. Pintauro, J.E. Haughan, E.A. Henning, J.L. Esterhai, T.P. Schaer, et al., Repair of dense connective tissues via biomaterial-mediated matrix reprogramming of the wound interface, Biomaterials 39 (2015) 85–94.
[8] S. Tarafder, J. Gulko, D. Kim, K.H. Sim, S. Gutman, J. Yang, et al., Effect of dose and release rate of CTGF and TGFbeta3 on avascular meniscus healing, J. Orthop. Res. 37 (7) (2019) 1555–1562.
[9] S. Tarafder, J. Gulko, K.H. Sim, J. Yang, J.L. Cook, C.H. Lee, Engineered healing of avascular meniscus tears by stem cell recruitment, Sci. Rep. 8 (1) (2018) 8150.
[10] M. Horie, M.D. Driscoll, H.W. Sampson, I. Sekiya, C.T. Caroom, D.J. Prockop, et al., Implantation of allogenic synovial stem cells promotes meniscal regeneration in a rabbit meniscal defect model, J Bone Joint Surg Am 94 (8) (2012) 701–712.
[11] F. Duygulu, M. Demirel, G. Atalan, F.F. Kaymaz, Y. Kocabey, T.C. Dulgeroglu, et al., Effects of intra-articular administration of autologous bone marrow aspirate on healing of full-thickness meniscal tear: an experimental study on sheep, Acta Orthop. Traumatol. Turcica 46 (1) (2012) 61–67.
[12] M. Horie, I. Sekiya, T. Muneta, S. Ichinose, K. Matsumoto, H. Saito, et al., Intra-articular Injected synovial stem cells differentiate into meniscal cells directly and promote meniscal regeneration without mobilization to distant organs in rat massive meniscal defect, Stem Cell. 27 (4) (2009) 878–887.
[13] Y. Nakagawa, T. Muneta, S. Kondo, M. Mizuno, K. Takakuda, S. Ichinose, et al., Synovial Mesenchymal Stem Cells Promote Healing after Meniscal Repair in Microminipigs. Osteoarthritis and Cartilage/OARS, Osteoarthritis Research Society, 2015.
[14] C.T. Jayasuriya, J. Twomey-Kozak, J. Newberry, S. Desai, P. Feltman, J.R. Franco, et al., Human cartilage-derived progenitors resist terminal differentiation and require CXCR4 activation to successfully bridge meniscus tissue tears, Stem Cell. 37 (1) (2019) 102–114.
[15] S.J. Heo, K.H. Song, S. Thakur, L.M. Miller, X. Cao, A.P. Peredo, et al., Nuclear softening expedites interstitial cell migration in fibrous networks and dense connective tissues, Sci. Adv. 6 (25) (2020), eaax5083.
[16] A.I. Bochynska, G. Hannink, R. Verhoeven, D.W. Grijpma, P. Buma, Evaluation of novel biodegradable three-armed- and hyper-branched tissue adhesives in a meniscus explant model, J. Biomed. Mater. Res., Part A 105 (5) (2017) 1405–1411.
[17] A.I. Bochynska, T.G. Van Tienen, G. Hannink, P. Buma, D.W. Grijpma, Development of biodegradable hyper-branched tissue adhesives for the repair of meniscus tears, Acta Biomater. 32 (2016) 1–9.
[18] S. Tarafder, G.Y. Park, J. Felix, C.H. Lee, Bioadhesives for musculoskeletal tissue regeneration, Acta Biomater. 117 (2020) 77–92.
[19] N. Gupta, M.A. Cruz, P. Nasser, J.D. Rosenberg, J.C. Iatridis, Fibrin-genipin hydrogel for cartilage tissue engineering in nasal reconstruction, Ann. Otol. Rhinol. Laryngol. 128 (7) (2019) 640–646.
[20] C. Ninh, A. Iftikhar, M. Cramer, C.J. Bettinger, Diffusion-reaction models of genipin incorporation into fibrin networks, J. Mater. Chem. B 3 (22) (2015) 4607–4615.
[21] G.D. Jay, K.A. Waller, The biology of lubricin: near frictionless joint motion, Matrix Biol. : journal of the International Society for Matrix Biology 39 (2014) 17–24.
[22] J.P. Gleghorn, A.R. Jones, C.R. Flannery, L.J. Bonassar, Boundary mode lubrication of articular cartilage by recombinant human lubricin, J. Orthop. Res. 27 (6) (2009) 771–777.
[23] Y. Lee, J. Choi, N.S. Hwang, Regulation of lubricin for functional cartilage tissue regeneration: a review, Biomater. Res. 22 (2018) 9.
[24] A.R. Jones, J.P. Gleghorn, C.E. Hughes, L.J. Fitz, R. Zollner, S.D. Wainwright, et al., Binding and localization of recombinant lubricin to articular cartilage surfaces, J. Orthop. Res. 25 (3) (2007) 283–292.
[25] D. Zhang, T. Cheriyan, S.D. Martin, A.H. Gomoll, T.M. Schmid, M. Spector, Lubricin distribution in the torn human anterior cruciate ligament and meniscus, J. Orthop. Res. 29 (12) (2011) 1916–1922.
[26] H. Majeed, S. Karuppiah, K.V. Sigamoney, G. Geutjens, R.G. Straw, All-inside meniscal repair surgery: factors affecting the outcome, J. Orthop. Traumatol. : official journal of the Italian Society of Orthopaedics and Traumatology 16 (3) (2015) 245–249.
[27] R.J. van der Wal, B.J. Thomassen, J.W. Swen, E.R. van Arkel, Time interval between trauma and arthroscopic meniscal repair has No influence on clinical survival, J. Knee Surg. 29 (5) (2016) 436–442.
[28] C.R. Flannery, R. Zollner, C. Corcoran, A.R. Jones, A. Root, M.A. Rivera-Bermúdez, et al., Prevention of cartilage degeneration in a rat model of osteoarthritis by intraarticular treatment with recombinant lubricin, Arthritis Rheum. 60 (3) (2009) 840–847.
[29] L.T. Senbanjo, M.A. Chellaiah, CD44: A Multifunctional Cell Surface Adhesion Receptor Is a Regulator of Progression and Metastasis of Cancer Cells, vol. 5, 2017, 18.
[30] Z. Cui, C. Xu, X. Li, J. Song, B. Yu, Treatment with recombinant lubricin attenuates osteoarthritis by positive feedback loop between articular cartilage and subchondral bone in ovariectomized rats, Bone 74 (2015) 37–47.
[31] D.K. Rhee, J. Marcelino, M. Baker, Y. Gong, P. Smits, V. Lefebvre, et al., The secreted glycoprotein lubricin protects cartilage surfaces and inhibits synovial cell overgrowth, J. Clin. Invest. 115 (3) (2005) 622–631.
[32] H. Zhu, N. Mitsuhashi, A. Klein, L.W. Barsky, K. Weinberg, M.L. Barr, et al., The role of the hyaluronan receptor CD44 in mesenchymal stem cell migration in the extracellular matrix, Stem Cell. 24 (4) (2009) 928–935.
[33] S. Tarafder, G. Park, C.H. Lee, Explant models for meniscus metabolism, injury, repair, and healing, Connect. Tissue Res. 61 (3–4) (2020) 292–303.
[34] M.B. Pabbruwe, W. Kafienah, J.F. Tarlton, S. Mistry, D.J. Fox, A.P. Hollander, Repair of meniscal cartilage white zone tears using a stem cell/collagen-scaffold implant, Biomaterials 31 (9) (2010) 2583–2591.
[35] A. Krych, Changing the Paradigm for Meniscal Injury Management: A Clinical Perspective, ORS webinar: Orthopaedic Research Society, 2016.
[36] O. Jeon, S.H. Ryu, J.H. Chung, B.S. Kim, Control of basic fibroblast growth factor release from fibrin gel with heparin and concentrations of fibrinogen and thrombin, J. Contr. Release 105 (3) (2005) 249–259.

[37] S.E. Sakiyama-Elbert, Incorporation of heparin into biomaterials, Acta Biomater. 10 (4) (2014) 1581–1587.

[38] H.S. Yang, W.G. La, S.H. Bhang, J.Y. Jeon, J.H. Lee, B.S. Kim, Heparin-conjugated fibrin as an injectable system for sustained delivery of bone morphogenetic protein-2, Tissue Eng. 16 (4) (2010) 1225–1233.

[39] S.A. Flowers, A. Zieba, J. Örnros, C. Jin, O. Rolfson, L.I. Björkman, et al., Lubricin binds cartilage proteins, cartilage oligomeric matrix protein, fibronectin and collagen II at the cartilage surface, Sci. Rep. 7 (1) (2017), 13149.

[40] A. Al-Sharif, M. Jamal, L.X. Zhang, K. Larson, T.A. Schmidt, G.D. Jay, et al., Lubricin/proteoglycan 4 binding to CD44 receptor: a mechanism of the suppression of proinflammatory cytokine-induced synoviocyte proliferation by lubricin, Arthritis Rheumatol. 67 (6) (2015) 1503–1513.

[41] S. Misra, V.C. Hascall, R.R. Markwald, S. Ghatak, Interactions between hyaluronan and its receptors (CD44, RHAMM) regulate the activities of inflammation and cancer, Front. Immunol. 6 (2015) 201.

[42] P.S. Raman, C.S. Alves, D. Wirtz, K. Konstantopoulos, Distinct kinetic and molecular requirements govern CD44 binding to hyaluronan versus fibrin(ogen), Biophys. J. 103 (3) (2012) 415–423.

[43] M.Y. Kwon, C. Wang, J.H. Galarraga, E. Puré, L. Han, J.A. Burdick, Influence of hyaluronic acid modification on CD44 binding towards the design of hydrogel biomaterials, Biomaterials 222 (2019), 119451.

[44] S.E. Majd, R. Kuijer, A. Köwitsch, T. Groth, T.A. Schmidt, P.K. Sharma, Both hyaluronan and collagen type II keep proteoglycan 4 (lubricin) at the cartilage surface in a condition that provides low friction during boundary lubrication, Langmuir : the ACS journal of surfaces and colloids 30 (48) (2014) 14566–14572.

[45] D.R. Hiscock, B. Caterson, C.R. Flannery, Expression of hyaluronan synthases in articular cartilage. Osteoarthritis and cartilage/OARS, Osteoarthritis Research Society 8 (2) (2000) 120–126.

[46] K. Matsumoto, Y. Li, C. Jakuba, Y. Sugiyama, T. Sayo, M. Okuno, et al., Conditional inactivation of Has2 reveals a crucial role for hyaluronan in skeletal growth, patterning, chondrocyte maturation and joint formation in the developing limb, Development 136 (16) (2009) 2825–2835.

[47] C.H. Lee, J.L. Cook, A. Mendelson, E.K. Moioli, H. Yao, J.J. Mao, Regeneration of articular surface of synovial joint by cell homing, Lancet 376 (9739) (2010) 440–448.

[48] C.H. Lee, F.Y. Lee, S. Tarafder, K. Kao, Y. Jun, G. Yang, et al., Harnessing endogenous stem/progenitor cells for tendon regeneration, J. Clin. Invest. 125 (7) (2015) 2690–2701.

[49] C.H. Lee, S.A. Rodeo, L.A. Fortier, C. Lu, C. Erisken, J.J. Mao, Protein-releasing polymeric scaffolds induce fibrochondrocytic differentiation of endogenous cells for knee meniscus regeneration in sheep, Sci. Transl. Med. 6 (266) (2014) 266ra171.

[50] C.H. Lee, B. Shah, E.K. Moioli, J.J. Mao, CTGF directs fibroblast differentiation from human mesenchymal stem/stromal cells and defines connective tissue healing in a rodent injury model, J. Clin. Invest. 120 (9) (2010) 3340–3349.

[51] C.H. Lee, N.W. Marion, S. Hollister, J.J. Mao, Tissue formation and vascularization in anatomically shaped human joint condyle ectopically in vivo, Tissue Eng. 15 (12) (2009) 3923–3930.

[52] S. Tarafder, A. Koch, Y. Jun, C. Chou, M.R. Awadallah, C.H. Lee, Micro-precise spatiotemporal delivery system embedded in 3D printing for complex tissue regeneration, Biofabrication 8 (2) (2016), 025003.

[53] R. Akhtar, N. Schwarzer, M.J. Sherratt, R.E. Watson, H.K. Graham, A.W. Trafford, et al., Nanoindentation of histological specimens: mapping the elastic properties of soft tissues, J. Mater. Res. 24 (3) (2009) 638–646.

[54] R. Yang, M. Chen, C.H. Lee, R. Yoon, S. Lal, J.J. Mao, Clones of ectopic stem cells in the regeneration of muscle defects in vivo, PLoS One 5 (10) (2010), e13547.